[Frontiers in Bioscience 10, 1290-1301 May 1, 2005]

MEMBRANE-PERMEABLE CYGNETS: RAPID CELLULAR INTERNALIZATION OF FLUORESCENT cGMP-INDICATORS

Akira Honda, Markus A. Moosmeier and Wolfgang R. Dostmann

Department of Pharmacology, University of Vermont, College of Medicine, Burlington, Vermont

TABLE OF CONTENTS

1. ABSTRACT

We have recently developed genetically encoded cGMP-indicators (cygnets) which have enabled us to study the spatial and temporal dynamics of intracellular cGMP in single cultured cells (1). However, primary mammalian cell types (dissociated cells or acute tissue samples) are often difficult to maintain undifferentiated in culture and the current established methods of introducing molecular reporters in single cells are laborious (micro-injection) and/or require cell culture techniques to accommodate the 1-2 day lag time of genetically mediated reporter expression. Here, we present an alternative, non-genetic method to rapidly introduce cGMP-indicators into cells and intact tissues using membrane permeable peptides (MPP). Five different 125 kDa MPP-cygnets were expressed and purified from insect SF9 cells. Three constructs showed high level cGMP-dependent FRET *in vitro*. One of the probes, Ant7-Cygnet, demonstrated emission ratio changes identical to the unmodified indicator. Ant7-Cygnet was rapidly (3 hours) and efficiently internalized in cultured smooth muscle cells and intact cerebral arteries. Furthermore, the internalized Ant7-Cygnet detected nitric oxide mediated elevations of intracellular cGMP in cultured smooth muscle cells and sensed increased levels of intracellular cGMP derived from C-type natriuretic peptide (CNP) induced guanylyl cyclase stimulation in intact arteries. These results demonstrate that MPP-cygnets provide a novel and potentially powerful technique to study intracellular cGMP in intact tissue.

2. INTRODUCTION

The second messenger guanosine 3',5'-cyclic monophosphate (cGMP) plays important roles in regulating various physiological processes in almost every tissue studied so far. Smooth muscle tone, neuronal excitability, epithelial electrolyte transport, phototransduction in the retina, and cell adhesion are just a few examples of cGMP's growing recognition in signal transduction (for reviews see 2-6). Highly dynamic and ephemeral in nature, cGMP transients are difficult to study due in part to a high degree of complexity in synthesis and degradation of the nucleotide by three distinct forms of guanylyl cyclases (7-9) and numerous phosphodiesterases (10), respectively. However, the major reason for our limited knowledge of cGMP function is a lack of techniques available to study cGMP in its native environment. Until recently, the only analytical methods available for studying cGMP included 1) radioimmunoassays, which require cell destruction and quantization of cGMP in terms of total protein content rather than free cGMP in individual cells (11); 2) immunohistochemistry, for the detection of cGMP in fixed tissue (12); and 3) patch cramming, a method of exposing cGMP-gated ion channels to the contents of disrupted cells to detect localized cGMP (13).

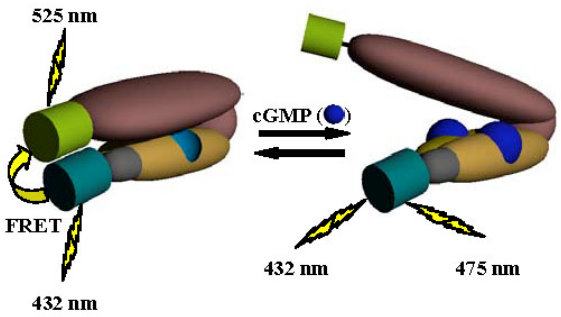

Figure 1. Model of FRET-based cGMP-indicators, Cygnets. A conformationally sensitive cGMP-binding fragment of PKG is sandwiched between enhanced versions of cyan and yellow fluorescence proteins (ECFP, ex. 432 nm, em. 475nm; citrine, ex. 480 nm, em. 525 nm) to modulate fluorescence resonance energy transfer (FRET) between the chromophores.

In order to study cGMP in single living cells we have created genetically encoded cGMP indicators that: (i) are sensitive and selective for cGMP; (ii) are easily incorporated into living cells by genetic transfection; (iii) are non-disruptive to intracellular signaling pathways; and (iv) utilize fluorescence detection to measure rapid cGMP transients (1, 14, 15). Cyclic-GMP-dependent protein kinase I alpha was chosen as the basis for the indicator because it is the most ubiquitous physiological sensor of cGMP, is not restricted to membranes, is related in structure to cAMP-dependent protein kinase from which indicators have already been engineered (16, 17), and is highly selective for cGMP over cAMP (18). Furthermore, PKG undergoes a relatively large conformational change upon cGMP binding (19) that is conducive to monitoring by fluorescence resonance energy transfer (FRET) between donor and acceptor fluorophores (figure 1). Our indicators, which we have called cygnets (cyclic GMP indicators using energy transfer) have enabled us to probe intracellular cGMP transients in response to physiological and pharmacological stimuli in a variety of cell types in unprecedented resolution and detail (1, 20).

Although we have developed novel genetically encoded cGMP-indicators, their application is limited to cultured cell lines. Current genetic delivery systems require at least 24 hours of incubation for cygnet expression. However, we need to establish an alternative method, which is able to deliver the indicators fast and efficiently. To resolve this conceptual stumbling block, we have designed new generation cygnets by fusion of membrane permeable peptides (MPP) to our cygnet constructs. We decided to genetically construct membrane permeable cygnets by attaching MPPs to the N-terminus of cygnets. Recently, we have utilized MPPs and developed a number of highly specific membrane permeable PKG inhibitors (21, 22). These fusion constructs demonstrated that PKG plays an important role in vascular tone (23). MPPs are arginine and lysine rich short peptides that mediate translocation across cellular membranes. MPPs have become widely used tools for the delivery of polynucleotides, small peptides, and proteins to cultured cells and even to living animal tissues (for reviews see 22, 24, 25, 26). These peptides were first found in the human immunodeficiency virus (HIV)-encoded transactivator of transcription (tat) protein (27). Further studies revealed that peptides derived from the Antennapedia transcription factor also have the capacity to mediate membrane translocation into cells (28). The precise mechanism of MPP-dependent membrane translocation is unclear. However, recent studies have suggested that cell surface glycosaminoglycans are required for MPP containing particle to associate with the cell surface and that protein translocation is mediated by a temperature-sensitive endocytosis mechanisms (29, 30).

Here we report the construction and functional purification of recombinant MPP-cygnets, characterize the functional utility of these novel cGMP-indicators *in vitro*, and demonstrate their feasibility as potential powerful tools for detecting intracellular cGMP transient in single smooth muscle cells in intact arterial tissue preparations.

3. MATERIALS AND METHODS

3.1. MPP-cygnet construction

Cygnet domain structure and genetic construction has been described previously (1). All sequences coding for membrane permeable peptides (MPPs) were fused to the 5'-end of the Cygnet-2.1 gene by one-sided overlap extension PCR. Peptide and DNA sequences for Ant16 (RQIKIWFQNRRMKWKK) and Ant7 (RRMKWKK) were from *Drosophila melanogaster* antennapedia hoemo-domain (P02833, GI: 45553294), tat13 (YGRKKRRQRRRPP) was obtained from the *HIV-1* transactivator of transcription protein and the oligomers Arg9 and Arg13 were generated according to mammalian codon usage. Forward primers were designed to contain MPPs and ECFP coding sequence in frame. The constructs that encode MPPs and ECFP were first amplified by PCR using an ECFP gene as a template and subsequently substituted for the original ECFP gene from Cygnet-2.1. All of the constructs were cloned into pFastBac (Invitrogen) vector for Sf9 cell expression.

3.2. Expression and purification

Sf9 cells were cultured in Sf-900 II SFM medium containing 2% FBS and 2% Pluronic F-68 (Sigma) in ambient air at 28 ºC and 115 rpm. High Five™ Tn5 cells were maintained in Express Five SFM medium containing 2% Pluronic F-68 under identical conditions. Sf9 cells and Tn5 cells were used for baculovirus infection and protein expression between passage numbers 3 and 12. All baculoviruses were amplified to approximately 1 x 10^9 pfu/ml titer for use in protein expressions. Sf9 cells were seeded at a cell density of 0.8 x 10^6 cells/ml 16-18 hours prior to infection with a 1:100 virus ratio at which point the cell density had reached 1.2-1.5 x 10^6 cells/ml. After 72 hours of incubation, cells were harvested by mild centrifugation (600g). MPP-cygnet protein expression levels were determined from the Sf9 cell pellets by western-blot analysis using a specific PKG type I antibody (Calbiochem). The MPP-cygnet/Sf9 cell pellets were resuspended in lysis buffer (50 mM potassium phosphate, pH 6.5, 10 mM DTT, 5mM EDTA, 5 mM EGTA, 10 mM

Table 1. MPP-cygnet solubility assays from Sf9 cell pellets. Recovery rate was examined by SDS-PAGE and 535 nm (Citrine) fluorescence intensity. Percent FRET were determined by 480/535 nm emission ratios

Additive	Conc. (%)	Recovery	Citrine intensity	FRET	Additive	Conc. (%)	Recovery	Citrine intensity	FRET
CHAPS	0.05	+	+	-	Pluronic F-68	1	+	++	++
	0.1	+	+	-		2	+	++	++
	1	+	+	-		5	+	++	++
Glycerol	10	+	++	+	SDS	0.05	+	+	-
	30	+	++	+		0.1	+	++	-
	50	+	+++	+		1	++	+	-
NaCl	0.05	-	+	-	Triton X-100	0.05	+	+++	-
	0.1	-	+	-		0.1	+	++	-
	1	-	++	-		1	+	+	-
PEG400	1	-	+/-	-	Urea	0.05	+	+++	+/-
	3	-	+/-	-		0.1	+	++	-
	5	-	+/-	-		1	+	+/-	-

benzamidine) including the protease inhibitor cocktail (50 microgram/ml TLCK, 100 microgram/ml TPCK, 100 microgram/ml SBTI, 170 microgram/ml PMSF, 50 microgram/ml antipain) and 5% Pluronic F-68 to a final ratio of 1 ml lysis buffer per gram wet cell pellet. Subsequent lysis using a French Pressure Cells at 1,200 psi and ultracentrifugation at 35,000 rpm for 45 min yielded clear to opaque supernatants, which were loaded onto 8-amino-ethylamino-cAMP agarose (8-AEA-cAMP) resins (Biolog, Germany). Columns were extensively washed with low and high salt (1 M NaCl) lysis buffers, and the proteins, clearly visible as a greenish band, were recovered from the column using a discontinuous and isocratic elution profile at room temperature with lysis buffer containing 1 mM cAMP. Pooled peak protein fractions were extensively dialyzed for 36 hours against 50 mM potassium phosphate, pH 6.8, 15 mM beta-mercaptoethanol, 1 mM EDTA, and 2 mM benzamidine.

3.3. Solubility assays

MPP-cygnet cell pellet aliquots were resuspended in lysis buffer containing protease inhibitors as described above. Additives were supplemented to the concentrations shown in table 1 and the mixture homogenized using a glass homogenizer. Samples were centrifuged at 14,000 rpm 4 °C for 15 minutes. Protein recovery was determined from the supernatants by SDS-PAGE (20 microgram per sample) and chemiluminescence-based PVDF Western-blotting and indicator function assessed by fluorescence spectroscopy (100 microgram per sample) by comparing the 432 nm and 480 nm excitation wavelengths with their corresponding emission wavelengths 480 nm and 535 nm, respectively.

3.4. *In vitro* fluorescence resonance energy transfer (FRET)

FRET measurements were performed using the Fluorescence Spectrometer F-4500 from Hitachi (Japan). Briefly, 50 nM MPP-cygnets were mixed with 50 mM potassium phosphate, 1 mM ATP, 2 mM $MgCl_2$, and different concentration of cGMP or cAMP. Samples were excited at 432 nm with PMT voltage at 700V and 5 nm slit width. Emission intensities were scanned between 450 nm and 580 nm at a scanning speed of 240 nm/min to minimize photobleaching. For every cyclic nucleotide titration the 480/535 nm FRET ratio was plotted against the concentration of cyclic nucleotide added to the sample and analyzed by Prism software (GraphPad, USA).

3.5. Cultured human mesenteric smooth muscle cells (HuMSM)

Human mesenteric and omental arteries were obtained from consenting surgical patients. This study used arteries taken from tissue specimens removed in conjunction with a planned surgical resection, primarily in individuals with either diverticulitis, Crohn's disease or ulcerative colitis. The University of Vermont has an approved assurance of compliance on file with the Department of Health and Human Services covering this activity (Assurance identification number: FWA727; IRB identification number: 485). Arteries were dissected in cold, oxygenated physiological salt solution (PSS) of the following composition (in mmol/L): 119 NaCl, 4.7 KCl, 24 $NaHCO_3$, 1.2 KH_2PO_4, 1.6 $CaCl_2$, 1.2 $MgSO_4$, 0.023 EDTA, 11 glucose (pH 7.4). After removing fat and connective tissue, isolated arteries were cut into 1-2 mm rings and embedded on a grid created on 60 mm cell culture dishes. The arterial segments were incubated with DMEM containing 10 % FBS, 50 microgram/ml gentamicin and 2.5 microgram/ml amphotericin B at 37 °C in humidified 5 % CO_2 until smooth muscle cells proliferated from the explant (7-10 days) (31). 80-90% confluent passage 1 cells (approximately 14 days after explant) cells were trypsinized, plated on glass-bottomed dishes and allowed to recover for 24 hours. MPP-cygnets were added to the culture media without FBS at a final concentration of 250 nM and incubated at 37 °C in humidified 5% CO_2 for 2-3 hours. Prior to imaging and FRET analysis cells were washed three times with PBS.

3.6. Cultured rat aortic smooth muscle cells (RaASM)

All animal use was performed according to the guidelines of the Institutional Animal Care and Use Committee of the University of Vermont. Mature Sprague-Dawley rats (250-350 g) were euthanized by lethal dose of pentobarbital and exsanguination. Thoracic aortas were carefully isolated to avoid strectching and cleaned by removing fat and connective tissue. Primary rat aortic smooth

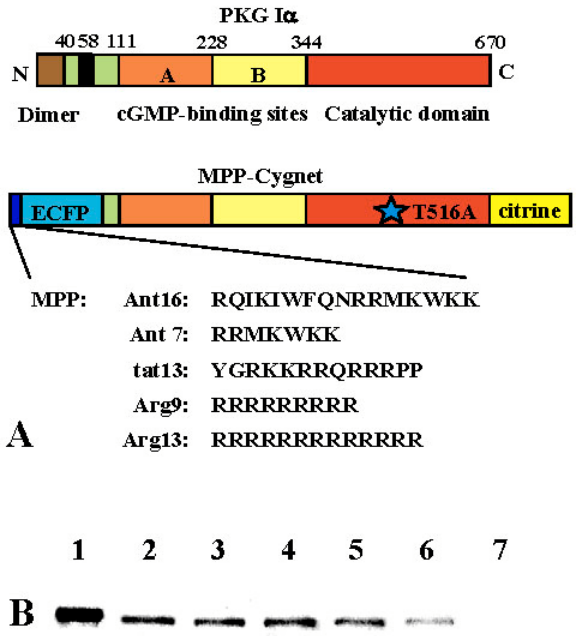

Figure 2. Membrane permeable peptides (MPP) sequences and domain structures of MPP-cygnets. (A) Five different MPPs were genetically attached to the N-terminus of Cygnet-2.1 (1). Ant16 and Ant7 peptides were taken from the Drosophila Antennapedia transcription factor sequence (aa43-58). TAT13 peptide was chosen from the HIV-encoded transactivator of transcription protein (aa47-59). R9 and R13 were derived from reports that poly-arginine peptides are capable of membrane translocation (39, 40, Dostmann, unpublished results). (B) Western blot of MPP-cygnet proteins expression in Tn5 cells. 20 microgram of cell extracts was used for SDS-PAGE. A PKG type I specific antibody probed proteins transferred on PVDF membrane. Lane 1, Purified Cygnet-2.1, 50 ng; lane 2, Ant16-Cygnet-2.1; lane3, Ant7-Cygnet-2.1; lane4, TAT13-Cygnet-2.1; lane5, R9-Cygnet-2.1; lane6, R13-Cygnet-2.1, lane7, mock-infected insect cell extract.

muscle cell cultures were generated by an adaptation of methods described by Berk and co-workers (32, 33). Briefly, arteries were incubated in Hank's Balanced Salt Solution (HBSS) supplemented with 1.25 U/ml elastase and 175 U/ml collagenase for 30-60 minutes in a shaking air incubator at 37 °C to allow for careful removal of the tunica adventitia. After the tunica media had been permitted to recover for 16-20 hours, smooth muscle cells were isolated by incubating 2-3 mm tissues pieces with HBSS containing 2.5 U/ml elastase and 175 U/ml collagenase for 1-2 hours and plated onto 60 mm culture dishes or glass bottom dishes. MPP-cygnet incubations were performed as mentioned above.

3.7. Rat cerebral arteries

Freshly isolated, intact basilar or cerebral arteries from euthanized Sprague-Dawley rat brains were incubated with 250 nM MPP-cygnets in serum-free DMEM culture media at 37 °C for 2 or 4 hours in humidified 5% CO_2. After washing three times with HBSS supplemented with 20 mM HEPES, 2 g/L glucose, arteries were cut longitudinally and fixed on a sylgard gel block (7x7x15 mm) with the lumen side exposed. The gel block had a 2-3 mm hole in the middle to gain access to the adventitial side. The complex was placed on thin (approximately 30 micrometer diameter) tungsten wires in glass bottom imaging dishes to create sufficient space for drug perfusion.

3.8. FRET imaging

MPP-cygnet treated cultured smooth muscle cells and small cerebral arteries (see above) were imaged using an inverted microscope (Nikon Diaphot 200) equipped with a 40/1.30 oil Ph4DL objective and ORCA ER cooled charge-coupled device camera (Hamamatsu; Bridgewater, NJ). All experiments were carried out in HBSS and 20 mM Hepes (pH 7.35), glucose (2 g/l). Dual-emission ratio imaging of the indicators was controlled by MetaFluor 4.64 software (Universal Imaging, West Chester, PA) using a 440DF20 excitation filter, a 455DRLP dichroic mirror, and two emission filters (480DF30 for ECFP, 535DF25 for EYFP and citrine) alternated by a filter changer (Lambda 10-2, Sutter Instruments, San Rafael, CA). Interference filters were obtained from Omega Optical and Chroma Technologies (Brattleboro, VT).

3.9. Confocal imaging

Rat cerebral arteries were analyzed using a Bio-Rad 2000 laser scanning confocal microscope (extation at 488 nm, emission at 535 nm for citrine). Identical settings (laser intensity, iris, and signal gain) were applied for assessment of MPP-cygnet treated and Cygnet-2.1 treated arteries.

3.10. Confocal 3D imaging

Confocal 3D images were recorded with a LSM 510 META detector system (Zeiss) on an inverted microscope Axiovert 200M using a PlanNeoFluar 40x, 1.4NA, oil immersion lens. CFP excitation with 405nm laser diode was at approximately 5% intensity and the emission captured using a 470-500 nm band. Z-stack dimensions were 230x230x67 micrometer, with pixel times every 3.2 microseconds and total acquisition time for the confocal image stack of 60 slices was 80 seconds. Images were processed and rendered using built-in functions of the Zeiss LSM software.

3.11. Materials

Insect Sf9 cells, High Five™ Tn5 cells, Sf-900 II SFM medium, Express Five SFM medium, and Bac-to-Bac expression system were obtained from Invitrogen (Carlsbad, CA). 8-AEA-cAMP resin affinity column, cGMP, cAMP were purchased from BioLog (Bremen, Germany). Digitonin, S-nitrosoglutathione (GSNO), (±)-S-nitroso-N-acetylpenicillamine (SNAP), C-type natriuretic peptide (CNP) and 3-isobutyl-1-methylxanthine (IBMX) were obtained from Calbiochem (La Jolla, CA). Gentamycin, Pluronic F-68 solution, L-1-chloro-3-(4-tosylamido)-7-amino-2-heptanone-HCL (TLCK), L-1-chloro-3-(4-tosylamido)-4-phenyl-2-butanone (TPCK), Soybean trypsin inhibitor (SBTI), phenylmethylsulfonyl fluoride (PMSF), benzamidine, dithiothreitol (DTT), and all other chemicals were purchased from Sigma (St. Louis, MO).

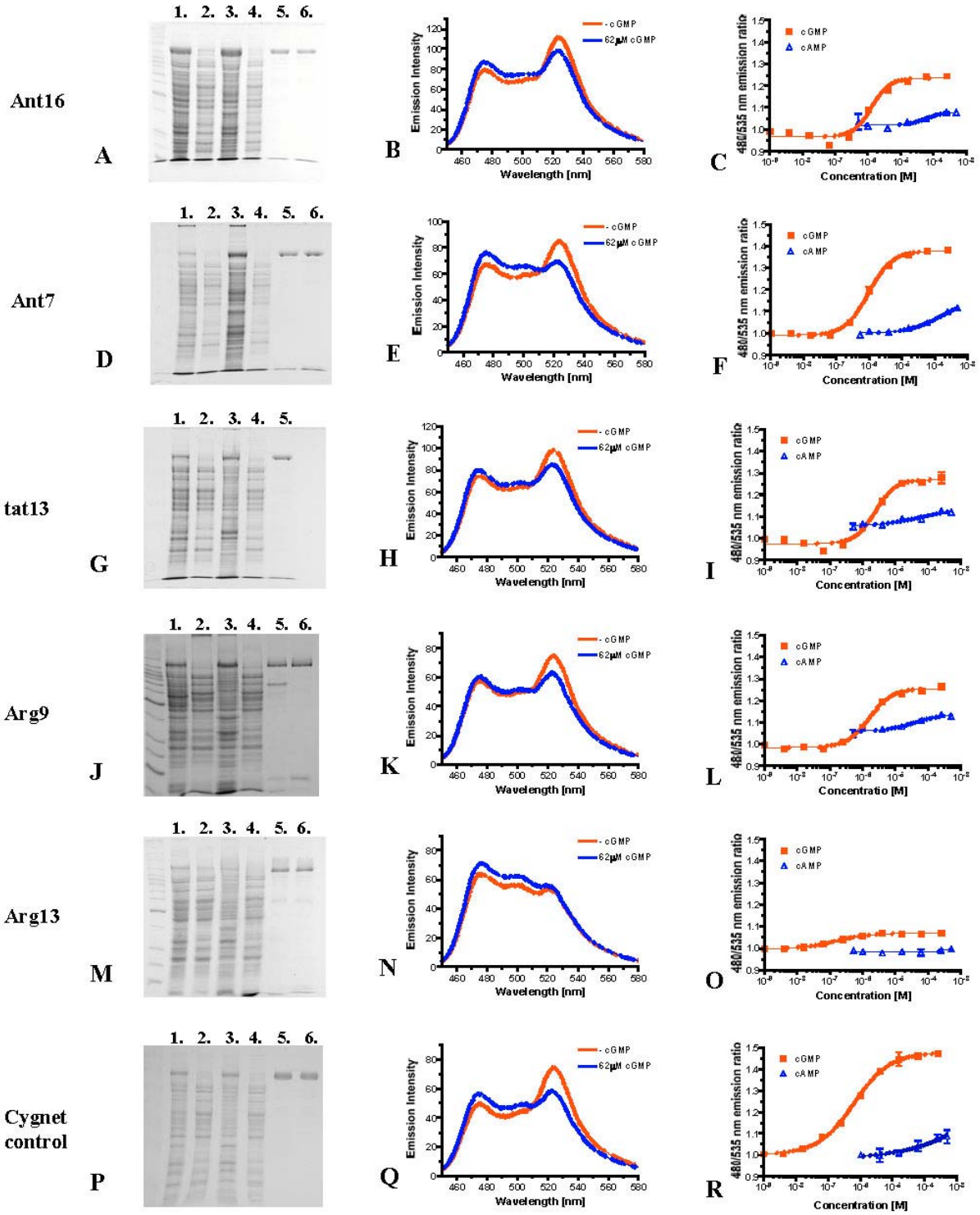

Figure 3. Purification, FRET analysis and cyclic nucleotide titration of recombinant MPP-cygnets Five different MPP-cygnets (Ant16-Cygnet: A-C, Ant7-Cygnet: D-F, TAT13-Cygnet: G-I, R9-Cygnet: J-L, R13-Cygnet: M-O, Cygnet-2.1: P-R) were expressed using the Sf9 cell/baculovirus system. (A, D, G, J, M, and P) 10% SDS-PAGE illustrating 8-AEA-cAMP-agarose affinity chromatography purification of the 124-kDa MPP-cygnets. Lanes 1, Sf9 cell homogenates; Lanes 2, soluble fractions; Lanes 3, insoluble fractions; Lanes 4, cAMP-agarose flow through fractions; Lanes 5, pooled 1 mM cAMP peak fractions; Lanes 6, fractions after dialysis. (B, E, H, K, N, and Q) Fluorescence spectra (excited at 432 nm) with zero and saturating cGMP (62 microM), respectively. (C, F, I, L, O, and R) FRET titration curves for cGMP and cAMP, combining three independent measurements.

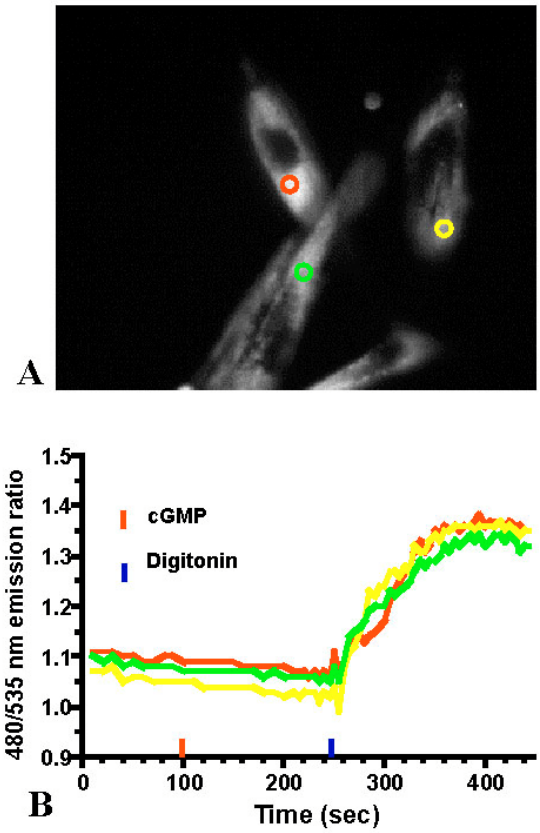

Figure 4. Ant7-MPP-cygnet internalization and *in vivo* fluorescence ratio imaging in cultured human mesenteric smooth muscle (HumSM) cells. (A) 40X, 485 nm emission image of HumSM cells incubated with 250 nM Ant7-Cygnet for three hours. Red, yellow and blue circles represent traces shown in (B). (B) FRET ratio traces during incubation with 50 microM cGMP for three minutes followed by 50 microM digitonin.

4. RESULTS

4.1. Purification and *in vitro* fluorescence resonance energy transfer

The construction of MPP-cygnets provided a number of experimental challenges. Although covalent linkage of medium size protein cargos to membrane permeable peptides has been reported previously (34, 35), with a mass of 124 KDa cygnets are the largest proteins ever attempted for intracellular delivery. We chose carrier sequences from the transactivator of transcription protein (tat13) (36), two MPP variants from the Drosophila Antennapedia homeo-domain (Ant16, Ant7) (37, 38) and two synthetic peptide derivatives with established membrane penetrating properties (39, 40, Dostmann, unpublished results). Next, a suitable expression system had to be identified and the recombinant indicators functionally purified. A major requirement for the development of these probes is that indicator fidelity should not be affected by the MPP fusion. In addition, the indicators need to be translocated efficiently into cells in culture and in intact tissue. Thirdly, the MPP-cygnets need to be functional as cGMP indicators once in the cytosol.

Five different MPP-cygnet fusion proteins were chosen and genetically constructed (figure 2A) using conventional PCR technology. All constructs were cloned in baculovirus and successfully expressed in insect cells (figure 2B). However, all of the expressed proteins were largely insoluble. Initial expression tests showed that treating cell pellets with additives known to increase protein solubility (table 1) proved to be more successful using Sf9 as opposed to Tn5 insect cells. Specifically, addition of 1-5% of the lipid Pluronic F-68 and to a lesser degree 10% glycerol to the lysis buffer markedly increased the soluble MPP-cygnet fractions during purification as summarized in table 1. We chose 5% Pluronic F-68 as additive for all MPP-cygnet preparations. Proteins were purified to apparent homogeneity using an cAMP-affinity chromatography approach for PKG (see Materials and Methods) as shown in figure 3 A, D, G, J, and M. Typical yields ranged from 2-3 mg soluble MPP-cygnet per liter Sf9 culture. Interestingly, the stability of MPP-cygnets was largely dependent on the concentration during storage. At concentrations below 1 mg/ml and 4 °C MPP-cygnets could be stored for several weeks (data not shown). Although, the stability of MPP-cygnets could be greatly enhanced at -20°C/50% glycerol, we only used freshly prepared indicators for all subsequent experiments.

To ascertain possible changes in FRET fidelity caused by the carriers, we performed a series of *in vitro* titrations. Figure 3 B, E, H, K, N and Q shows fluorescence spectra (excited at 430 nm) with zero and saturating (30 microM) cGMP, respectively. A hallmark of cygnet emission spectra (figure 3 Q) is the profound YFP emission intensity (1). Although all MPP-cygnets decreased FRET upon saturation with cGMP, resulting in an increase of cyan to yellow emission ratios, the poly-arginine carrier Arg13 showed a marked decrease in YFP emission. Apparently, the poly Arg-fusion interrupts efficient energy transfer between the chromophores. Further analysis of all constructs confirmed that neither of the poly-Arg MPPs (Arg13 or Arg9) were suitable for cygnet function. As figures 3 C, F, I, L, O and R illustrate the cGMP/cAMP titration curves of the emission ratios for MPP-cygnets differ remarkably. Fluorescence spectra were recorded in the presence of increasing concentrations of cGMP or cAMP and the FRET ratio calculated. Table 2 summarizes the results. Although Ant16-, Ant7- and Tat13-Cygnet showed similar profiles of cGMP FRET ratio changes, we chose Ant7-Cygnet for all subsequent studies. Ant7-Cygnet, of all constructs displayed the most similar cGMP and cAMP titration curves compared to Cygnet-2.1 (figure 3F, R; table 2).

4.2. Translocation and *in vivo* FRET in cultured smooth muscle cells

Next, we examined the ability of Ant7-cygnet to translocate into cultured smooth muscle cells. Figure 4A demonstrates the indicator's uptake in early passage human mesenteric arterial smooth muscle cells. Incubation conditions (250 nM of MPP-cygnet proteins, 3 hours at 37ºC) were kept constant throughout the experiments and

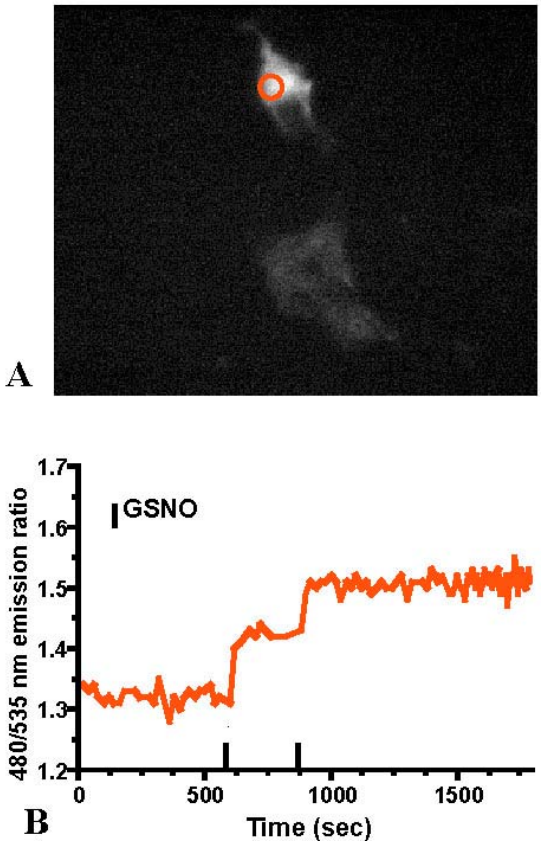

Figure 5. Pharmacological modulation of cGMP in human mesenteric smooth muscle cells. (A) 485 nm emission image of Ant7-Cygnet (250 nM, 3 hours) treated HumSM cells. (B) 20 second interval FRET ratio recording corresponding to the red circled region depicted in (A). The NO donor (GSNO) elicited a 15% FRET ratio increase in the presence of 0.6 mM IBMX.

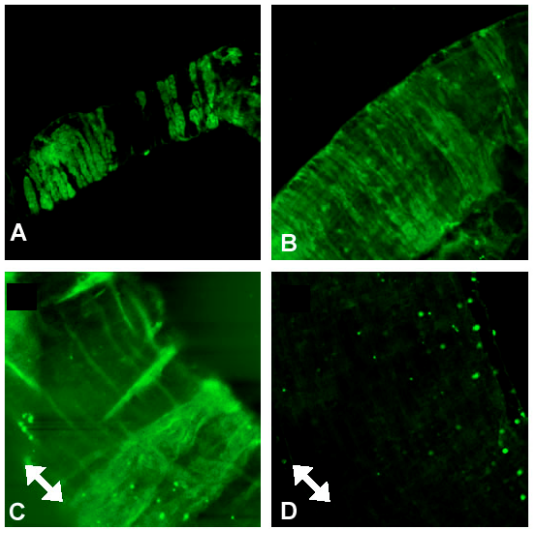

Figure 6. MPP-cygnet internalization in intact rat cerebral arteries. Cerebral arteries from rat were incubated with Ant7-Cygnet (A & B), Ant16-Cygnet (C) or Cygnet-2.1 control (D) for three hours. Samples were excited at 480 nm and YFP emission detected at 530 nm and then applied to confocal imaging. White arrows indicate longitudinal orientation of arteries.

cells were monitored by fluorescence imaging. Strikingly, the majority of cells had internalized the indicator, which showed relatively even cytosolic distribution and nuclear exclusion, as was expected for a 125 KDa protein containing no nuclear translocation signal sequence. To verify indicator uptake and cGMP-indicator activity *in vivo,* cells were first incubated with cGMP and subsequently treated with digitonin (figure 4 B). Extracellular cGMP failed to elicit a response, indicating that Ant7-Cygnet had indeed internalized and was not merely deposited on the cellular membrane. After digitonin treatment (1 min.) compromised the cellular membrane integrity, extracellular cGMP was able to freely enter the cells and induce a 30% ratio change. Application of digitonin alone had no effect on FRET (data not shown). These results indicate that Ant7-Cygnet readily translocates into cultured cells and retains its function as a cGMP-indicator once inside the cells.

Subsequently we investigated whether Ant7-Cygnet was capable of detecting a physiological cGMP increase in response to nitric oxide induced soluble guanylyl cyclase stimulation. Again, we used smooth muscle cells from human mesenterium and the results are illustrated in figure 5. After inhibiting phosphodiesterase (PDE) activity with 0.6 mM IBMX, repeated application of the NO donor GSNO (100 microM) increased the emission ratio stepwise by a total of 25% (figure 5 B). We conclude that cell-penetrating MPP-cygnets are functional and effective as intracellular cGMP-indicators in both *in vitro* and *in vivo* conditions.

4.3. Functional MPP-Cygnet delivery in smooth muscle cells of intact cerebral arteries

After we demonstrated that Ant7-Cygnet can translocate and is functional as a cGMP-indicator in cultured cells, we proceeded to test the utility of this MPP-cygnet in smooth muscle cells in intact vessels. Small cerebral arteries from rat were incubated for 3 hours with Ant7-Cygnet and Ant16-Cygnet as described in *Material and Methods* and indicator internalization visualized by confocal fluorescence imaging. As shown in figure 6, both MPP-cygnets were able to translocate into cerebral smooth muscle cells and both indicators were evenly distributed in the cytosol. However, indicator delivery appeared to be somewhat patchy. In contrast, no specific uptake was detected in rat cerebral arteries incubated of with Cygnet-2.1 protein (no MPP) under identical conditions (figure 6 D), indicating that successful internalization is a specific result of the MPP sequences.

To further probe the translocation abilities and spectral properties of MPP-Cygnets, we performed three dimensional confocal analyses of Ant7-Cygnet treated arteries using the LSM 510 META system from Zeiss (figure 7). First, we confirmed fluorescence energy transfer by exciting a 11-16 micrometer slice within the media of the artery at 458 nm and monitoring the CFP emission at 480 nm and the Citrine emission at 530 nm of individual smooth muscle cells as shown in figure 7 A. Emission spectra of Ant7-Cygnet taken from various intracellular regions of smooth muscle cells were undistinguishable

Table 2. Kinetic analysis of MPP-cygnets *in vitro*. All data were generated from three independent experiments and expressed as mean ± SEM

MPP-cygnet	Max. % $FRET_{cGMP}$	Max. % $FRET_{camp}$	App. $K_{D,cGMP}$ [µM]	App. $K_{D,cAMP}$ [µM]	cGMP selectivity
Ant16	24.6±0.98	7.7±0.67	1.3±0.060	60.9±0.33	48
Ant7	38.4±0.36	11.6±0.32	0.96±0.050	≥250	≥260
tat13	27.8±3.22	11.8±0.98	2.4±0.063	68.0±0.75	29
Arg9	26.5±1.47	13.5±1.47	1.6±0.046	38.2±0.32	24
Arg13	7.1±0.11	0.1±0.44	0.15±0.011	N.D.	N.D.
Cygnet-2.1	47.3±0.02	9.2±0.9	0.64±0.063	≥250	≥400

from the *in vitro* spectrum shown in figure 3 E (data not shown). Next, a 1-30 micrometer confocal z-stack (1 micrometer segments) of the whole artery was converted into an integrated color depth projection (figure 7B). Endothelial cells and smooth muscle cells were easily identified by their anti-parallel orientation. These results demonstrate that Ant7-Cygnet internalizes in all cell types found in cerebral arteries.

Our findings presented above encouraged us to explore experimental conditions that might allow us to monitor intracellular cGMP levels in individual smooth muscle cells in intact arteries using emission ratio imaging. Ant7-Cygnet treated basilar brain arteries from rat were cut longitudinally and attached to a Sylgard^{TM} gel cube with the lumen exposed. A hole had been cut in the gel cube to allow access not only to the luminal side, but to the advential side of the artery as well. Figure 8 A shows concentrated indicator translocation in the media (arrows depict individual smooth muscle cells) of arteries incubated for 3 hours incubation with Ant7-Cygnet. Again, the indicator was distributed evenly in the cytosol and showed nuclear exclusion. As shown in figure 8 C and D defined regions of individual cells were imaged with ECFP excitation at 430 nm and emissions were monitored at 480 nm and 535 nm every ten seconds. Given a high background fluorescence the starting 480/535 nm emission ratios were comparatively high (1.4-1.5, figure 8 D). However, we observed approximately 15% FRET ratio changes when cGMP synthesis was stimulated through C-type natriuretic peptide (CNP) mediated activation of the particulate guanylyl cyclase (figure 8 D). We observed these responses to CNP without any PDE inhibition. However the nitric oxide donor, SNAP (±IBMX) failed to elicit a response. This may be due to the high fluorescence background at which NO mediated cGMP transients become very difficult to detect.

5. DISCUSSION

The need for alternative techniques to introduce molecular probes in cells of cultured intact tissues becomes apparent when one recognizes that often key intracellular signaling mechanisms are difficult to maintain in the cell type of interest (41, 42, 43). In the case of small arteries from rat brain we have recently shown that the expression of cGMP-dependent protein kinase, a key component of the nitric oxide induced vasodilation signaling cascade, is substantially down regulated in organ culture (23).

We propose that the development of MPP-cygnets is likely to advance the concept of protein transduction for a number of reasons. First, intracellular indicator delivery is achieved within 2-3 hours allowing measurements in native, non-cultured tissue. Also, indicator distribution is cytosolic with minimal clustering and organelle/membrane association. Thirdly, select MPP-cygnets possess superb selectivity and sensitivity as cGMP-indicators, and lastly, the use of membrane permeable peptides as carriers for large, >100 kDa protein cargos as probes for intracellular messenger molecules has now become possible. We chose N-terminal linkage of MPPs to minimize indicator disturbance, with five established carrier sequences (24, 26), which we used successfully in our previous work (figure 2) (21, 22, 23).

Although indicator design was relatively straight forward, we needed to overcome several difficult experimental hurdles to prove MPP-cygnet feasibility as indicators in cells of intact tissues. First, MPP-cygnets had to be expressed as soluble and functional intact proteins. Solubility was a serious concern, since MPPs are known to associate with the cellular membranes (44). However, the utilization of a lipid-based protocol in combination with the Sf9 insect cell expression system provided the means to obtain reasonable yields of all indicators used in this study (table 1). It should be noted that Pluronic F-68 showed the highest rate of recovery from a number of different lipids (data not shown). However, a large fraction of the expressed indicators still remained insoluble. The five different MPP constructs displayed noticeably different emission ratio properties upon analysis of their fluorescence spectra (figure 3, table 2). In comparison to Cygnet-2.1, only Ant16-, Ant7-, and Tat13-Cygnet showed similar cGMP dependent 480/535 nm ratio changes. However, the cAMP titration curves of Ant16- and Tat13-Cygnet resulted in lower cGMP/cAMP selectivities. Only Ant7-Cygnet was analogous to Cygnet-2.1 in every aspect of our spectral analyses (figure 3, table 2). The fact that Ant7 is the shortest of the five MPP sequences (figure 2) suggests that cygnet function may be sensitive to changes of its electrostatic environment. Energy transfer was nearly abolished in the largest and highly charged MPP Arg13-Cygnet (figure 3 N, O).

After Ant7-Cygnet was identified as our best candidate, we needed to show that the indicator was capable of cellular translocation and that once inside mammalian cells, was fully functional as cGMP-indicator. An incubation period of three hours was sufficient to observe efficient and primarily cytosolic cellular indicator delivery (figure 4, 5). To date, we have not investigated in detail the time and concentration dependency of MPP-cygnet internalization. However, 3 hours incubation and

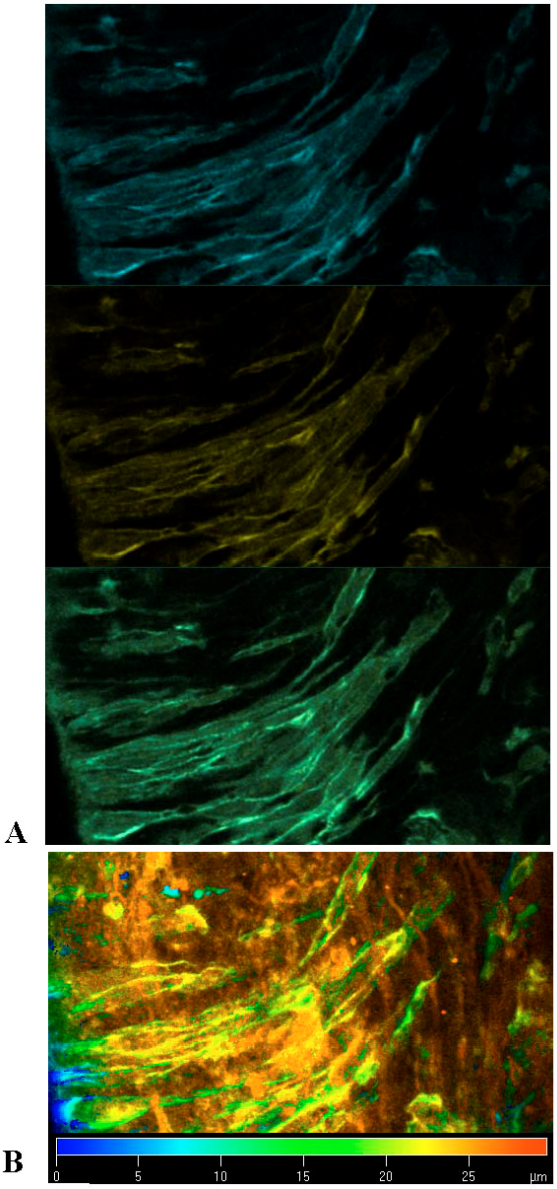

Figure 7. Three dimensional depth projection of medial Ant7-Cygnet translocation. (A) 11-16 micrometer splitview of smooth muscle cells within an arterial segment from rat cerebrum treated with Ant7-Cygnet (250 nM, 3 hours). The sample was excited at 458 nm and the emission intensities were captured at 480 (CFP-blue) and 530 nm (Citrine-yellow; composite-green). (B) Integrated color depth coding of the 1-30 micrometer confocal z-stack (458 nm excitation). Images were taken with Zeiss confocal microscope LSM 510 META and processed using built-in functions of the Zeiss LSM software.

250 nM indicator concentration may be near optimal; higher concentrations showed considerably more punctuate indicator distribution (data not shown). Using these conditions, we found precisely the same cellular distribution as for cultured smooth muscle cells transfected with cygnet-DNA. We conclude that purified MPP-cygnets have the ability to non-destructively translocate the plasma membrane of cultured smooth muscle cells. In addition, Ant7-Cygnet intracellular function was verified using a nitric oxide donor (GSNO) as a physiological stimulus (figure 5). Repeated 100 microM GSNO application resulted in incremental increases of cGMP. In some instances single applications of the NO donor or natriuretic peptides elicited maximal responses which were not increased further with additional stimulations (data not shown). The experiments outlined in figure 4 demonstrated that the indicator was actually cytosolic and not simply deposited on the cellular surface. It should be noted that digitonin can lyse smooth muscle cells, usually within 1-2 minutes. However, this short period apparently is sufficient for extracellular cGMP to diffuse in the cells and elicit a strong emission ratio change prior to cell lysis.

Finally, MPP-cygnet function had to be established in intact tissue. We chose small cerebral arteries from rat for the following reasons; (i) we wanted to expand our smooth muscle cell culture model to smooth muscle cells in tissue, (ii) these arteries consist to >90% of smooth muscle, and (iii) the adventia is relatively thin and surrounding connective tissue can be easily removed. Thus indicator delivery was possible not just through the lumen but through the advential side. This may explain the erratic staining pattern shown in figure 6. Incomplete removal of connective tissue may have caused less effective penetration of the indicator through the advential side during the three hour incubation time, or fat from connective tissue may absorb significant amounts of the MPP-cygnets before the indicators reach the medial layer.

To examine the extent of MPP-cygnet uptake across the arterial wall, we employed the LSM 510 META confocal microscope system (Zeiss) and generated a series of 3D-depth projections of arterial segments. As figure 7 demonstrates, the medial cell layer is clearly distinguishable from the endothelium, both of which are evidently marked by the indicator Ant7-Cygnet. Again, indicator distribution appears to be uneven with single cells clearly prominent (figure 7 A). This property of Ant7-Cygnet served to our advantage in selecting individual cells for ratiometric imaging. However, we have yet to identify preparation conditions under which even localization of cygnet delivery can be attained. We are currently investigating the tissue specific kinetics of MPP-cygnet uptake.

Finally, we attempted to measure cGMP in response to physiological stimuli in single smooth muscle cells within arterial segments. Initial experiments using whole arteries failed, due to high background fluorescence (figure 8). Only when the media was flattened by cutting the arteries longitudinally and fixing segments on sylgard gel blocks, individual smooth muscle could be screened for cGMP transients. Although the cGMP response trace shown in figure 8 D is clearly approaching the limit of our current epi-flourescence ratiometric imaging set-up, C-type natriuretic peptide (CNP) showed approximately a 15% ratio change. These results are in accordance with our previous data obtained with smooth muscle cells transiently transfected with Cygnet-2.1 (14). Apparently, activation of

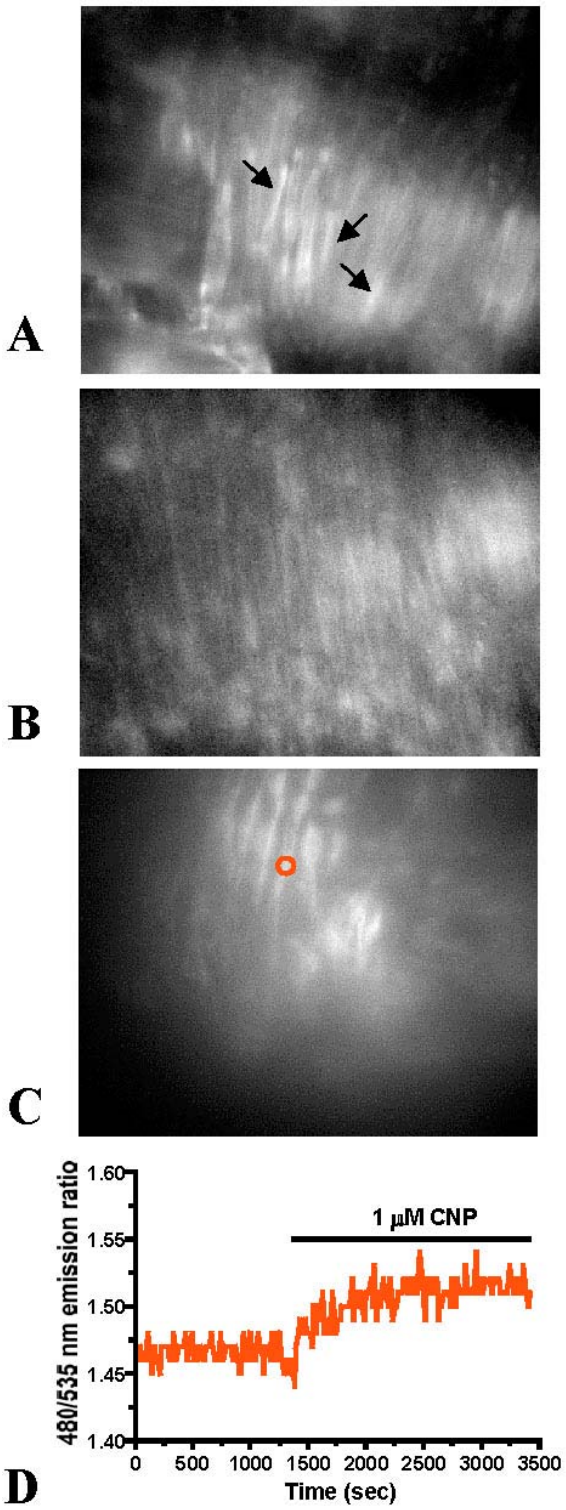

Figure 8. *Imaging of cGMP in smooth muscle cells in arteries*. (A-C) Fluorescence images (40X) of smooth muscle cells (arrows) within the medial layer of Ant7-Cygnet treated basilar artery segments (endothelium facing outward). Red circle depicts the area used for FRET ratio recording as shown in D. (D) 480/535 nm emission ratio responding to 1 microM CNP in the absence of IBMX.

particulate guanylyl cyclase (GC-A and GC-B) activity elicits robust and highly reproducible cGMP in smooth muscle. In contrast, nitric oxide induced cGMP transients are less stable and their kinetic behavior can change widely (45, 46). So far, we have not been able to obtain reproducible NO mediated cGMP transients using Ant7-Cygnet in intact tissue. We are currently implementing new confocal FRET technology (Zeiss) to further analyse this experimental cGMP monitoring system. However, MPP-cygnets have the potential to revolutionize not only our methods of cellular indicator delivery but our understanding of cGMP signaling under physiological conditions.

6. ACKNOWLEDGEMENTS

We thank Drs. Neil Hyman in the Department of Surgery and George Wellman, Department of Pharmacology for making human tissue samples available to us. Dr. Mark Taylor, Sharon Cawley and Kristina Laskovski provided assistance with the tissue culture and preparation of rat cerebral arteries. We thank Sebastian Tille, Zeiss for confocal image acquisition and 3D data processing and Christian Nickl for art work. This work was supported by the National Science Foundation (MCB-9983097), the Lake Champlain Cancer Research Organization and the Totman Medical Research Trust (to W.R.D.)' with this sentence: "This work was supported by the National Science Foundation (MCB-9983097), National Institute of Health (HL68991) and the Lake Champlain Cancer Research Organization and the Totman Medical Research Trust (to W.R.D.).

7. REFERENCES

1. Honda A, S. R. Adams, C. L. Sawyer, V. Lev-Ram, R. Y. Tsien and W. R. G. Dostmann: Spatiotemporal dynamics of guanosine 3',5'-cyclic monophosphate revealed by a genetically encoded, fluorescent indicator. *Proc Natl Acad Sci USA* 98, 2437-2442 (2001)

2. Schlossmann J, R. Feil and F. Hofmann: Signaling through NO and cGMP-dependent protein kinases. *Ann Med* 35, 21-27 (2003)

3. Lincoln T. M, N. Dey and H. Sellak: cGMP-dependent protein kinase signaling mechanisms in smooth muscle: from the regulation of tone to gene expression. *J Appl Physiol* 91, 1421-1430 (2001)

4. Kuhn M: Structure, regulation, and function of mammalian membrane guanylyl cyclase receptors, with a focus on guanylyl cyclase-A. *Circ Res* 93, 700-709 (2003)

5. Kaupp U. B and R. Seifert: Cyclic nucleotide-gated ion channels. *Physiol Rev* 82, 769-824 (2002)

6. Feil R, S. M. Lohmann, H. de Jonge, U. Walter and F. Hofmann: Cyclic GMP-dependent protein kinases and the cardiovascular system: insights from genetically modified mice. *Circ Res* 93, 907-916 (2003)

7. Wedel, B and D. Garbers: The guanylyl cyclase family at Y2K. *Ann Rev Physiol* 63, 215-233 (2001)

8. Krumenacker J. S, K. A. Hanafy and F. Murad: Regulation of nitric oxide and soluble guanylyl cyclase. *Brain Res Bull* 62, 505-515 (2004)

9. Hamad A. M, A. Clayton, B. Islam and A. J. Knox: Guanylyl cyclases, nitric oxide, natriuretic peptides, and airway smooth muscle function. *Am J Physiol Lung Cell Mol Physiol* 285, L973-983 (2003)

10. Rybalkin S. D, C. Yan, K. E. Bornfeldt and J. A. Beavo: Cyclic GMP phosphodiesterases and regulation of smooth muscle function. *Circ Res* 93, 280-291 (2003)

11. Steiner A. L, R. E. Wehmann, C. W. Parker and D. M. Kipnis: Radioimmunoassay for the measurement of cyclic nucleotides. *Adv Cyclic Nucleotide Res* 2, 51-61 (1972)

12. Barsony J and S. J. Marx: Immunocytology on Microwave-Fixed Cells Reveals Rapid and Agonist-Specific Changes in Subcellular Accumulation Patterns for cAMP or cGMP. *Proc Natl Acad Sci USA* 87, 1188-1192 (1990)

13. Kramer R. H: Patch cramming: monitoring intracellular messengers in intact cells with membrane patches containing detector ion channels. *Neuron* 4, 335-341 (1990)

14. Sawyer C. L, A. Honda and W. R. G. Dostmann: Cygnets: spatial and temporal analysis of intracellular cGMP. *Proc West Pharmacol Soc* 46, 28-31 (2003)

15. Sawyer C. L, A. Honda and W. R. G. Dostmann: Cygnets: intracellular cGMP sensing in primary cells using fluorescence energy transfer. *Cell Biology, in press* (2004)

16. Adams S. R, A. T. Harootunian, Y. J. Buechler, S. S. Taylor and R. Y. Tsien: Fluorescence ratio imaging of cyclic AMP in single cells. *Nature* 349, 694-697 (1991)

17. Zaccolo M, F. De Giorgi, C. Y. Cho, L. Feng, T. Knapp, P. A. Negulescu, S. S. Taylor, R. Y. Tsien and T. Pozzan: A genetically encoded, fluorescent indicator for cyclic AMP in living cells. *Nat Cell Biol* 2, 25-29 (2000)

18. Ruth P, W. Landgraf, A. Keilbach, B. May, C. Egleme and F. Hofmann: The activation of expressed cGMP-dependent protein kinase isozymes I alpha and I beta is determined by the different amino-termini. *Eur J Biochem* 202, 1339-1344 (1991)

19. Zhao J, J. Trewhella, J. Corbin, S. Francis, R. Mitchell, R. Brushia and D. Walsh: Progressive cyclic nucleotide-induced conformational changes in the cGMP-dependent protein kinase studied by small angle X-ray scattering in solution. *J Biol Chem* 272, 31929-31936 (1997)

20. Honda A, C. L. Sawyer, S. M. Cawley and W. R. G. Dostmann: Cygnets: *in vitro* characterization of novel cGMP indicators and *in vivo* imaging of intracellular cGMP. *Methods in Molecular Biology*, *in press* (2004)

21. Dostmann W. R. G, C. K. Nickl, M. S. Taylor, J. E. Brayden, R. Frank and W. J. Tegge: Highly specific, membrane-permeant peptide blockers of cGMP-dependent protein kinase Ialpha inhibit NO-induced cerebral dilation. *Proc Natl Acad Sci USA* 97, 14772-14777 (2000)

22. Dostmann W. R. G, W. Tegge, R. Frank, C. K. Nickl, M. S. Taylor and J. E. Brayden: Exploring the mechanisms of vascular smooth muscle tone with highly specific, membrane-permeable inhibitors of cyclic GMP-dependent protein kinase Ialpha. *Pharmacology and Therapeutics* 93, 203-215 (2002)

23. Taylor M. S, C. Okwuchukwusanya, C. K. Nickl, W. Tegge, J. E. Brayden and W. R. G. Dostmann: Inhibition of cGMP-dependent protein kinase by the cell-permeable peptide DT-2 reveals a novel mechanism of vasoregulation. *Mol Pharmacol* 65, 1111-1119 (2004)

24. Joliot A and A. Prochiantz: Transduction peptides: from technology to physiology. *Nature Cell Biol* 6, 189-196 (2004)

25. Futaki S, S. Goto and Y. Sugiura: Membrane permeability commonly shared among arginine-rich peptides. *J Mol Recognit* 16, 260-264 (2003)

26. Lundberg P and U. Langel: A brief introduction to cell-penetrating peptides. *J Mol Recognit* 16, 227-233 (2003)

27. Mann D. A and A. D. Frankel: Endocytosis and targeting of exogenous HIV-1 Tat protein. *EMBO J* 10, 1733-1739 (1991)

28. Schwarze S. R, K. A. Hruska and S. F. Dowdy: Protein transduction: unrestricted delivery into all cells? *Trends Cell Biol* 10, 290-295 (2000)

29. Console S, C. Marty, C. Garcia-Echeverria, R. Schwendener and K. Baller-Hofer: Antennapedia and HIV transactivator of transcription (TAT) "protein transduction domains" promote endocytosis of high molecular weight cargo upon binding to cell surface glycosaminoglycans. *J Biol Chem* 278, 35109-35114 (2003)

30. Belting M: Heparan sulfate proteoglycan as a plasma membrane carrier. *Trends Biochem Sci* 28, 145-151 (2003)

31. Cornwell T. L and T. M. Lincoln: Regulation of intracellular Ca^{2+} levels in cultured vascular smooth muscle cells: reduction of Ca^{2+} by atriopeptin and 8-bromo-cyclic GMP is mediated by cyclic GMP-dependent protein kinase. *J Biol Chem* 264, 1146-1155 (1989)

32. Travo P, G. Barret and G. Burnstock: Differences in proliferation of primary cultures of vascular smooth muscle cells taken from male and female rats. *Blood Vessels* 17, 110-116 (1980)

33. Korshunov V. A and B. C. Berk: Flow-induced vascular remodeling in the mouse: a model for carotid intima-media thickening. Arterioscler. Thromb. *Vasc Biol* 23, 2185-2191 (2003)

34. Cao G, W. Pei, H. Ge, Q. Liang, Y. Luo, F. R. Sharp,

A. Lu, R. Ran, S. H. Graham and J. Chen: *In vivo* delivery of a Bcl-xL fusion protein containing the TAT protein transduction domain protects against ischemic brain injury and neural apoptosis. *J Neuroscience* 22, 5423-5431 (2002)

35. Zoog S. J, V. V. Papov, S. S. Pullen, S. Jakes and M. R. Kehry: Signaling and protein association of a cell permeable CD40 complex in B cells. *Molecular Immunology* 40, 681-694 (2004)

36. Frankel, A. D. and C. O. Pabo: Cellular uptake of the Tat protein from human immunodeficiency virus. *Cell* 55, 1189–1193 (1988)

37. Derossi D, A. H. Joliot, G. Chassaing and A. Prochiantz: The third helix of the Antennapedia homeodomain translocates through biological membranes. *J Biol Chem* 269, 10444-10450 (1994)

38. Fischer P. M, N. Z. Zhelev, S. Wang, J. E. Melville, R. Fahreus and D. P. Lane: Structure-activity relationship of truncated and substituted analogues of the intracellular delivery vector penetratin. *J Peptide Res* 55, 163-172 (2000)

39. Wender P. A, D. J. Mitchell, K. Pattabiraman, E. T. Pelkey, L. Steinman and J. B. Rothbard: The design, synthesis, and evaluation of molecules that enable or enhance cellular uptake: peptoid molecular transporters. *Proc Natl Acad Sci USA* 97, 13003-13008 (2000)

40. Mitchell D. J, D. T. Kim, L. Steinman, C. G. Fathman and J. B. Rothbard: Polyarginine enters cells more efficiently than other polycationic homopolymers. *J Pept Res* 56, 318-325 (2000)

41. Li S, J. J. Moon, H. Miao, G. Jin, B. P. Chen, S. Yuan, Y. Hu, S. Usami and S. Chien: Signal transduction in matrix contraction and the migration of vascular smooth muscle cells in three-dimensional matrix. *J Vasc Res* 40, 378-388 (2003)

42. Matsubara S and M. Ozawa: Expression of alpha-catenin in alpha-catenin-deficient cells results in a reduced proliferation in three-dimensional multicellular spheroids but not in two-dimensional monolayer cultures. *Oncogene* 23, 2694-2702 (2004)

43. Bouhadir K. H and D. J. Mooney: *In vitro* and *in vivo* models for the reconstruction of intercellular signaling. *Ann NY Acad Sci* 842, 188-194 (1998)

44. Vives E, P. Brodin and B. Lebleu: A truncated HIV-1 Tat protein basic domain rapidly translocates through the plasma membrane and accumulates in the cell nucleus. *J Biol Chem* 272, 16010-16017 (1997)

45. Mullershausen F, A. Friebe, R. Feil, W. J. Thompson, F. Hofmann and D. Koesling: Direct activation of PDE5 by cGMP: long-term effects within NO/cGMP signaling. *J Cell Biol* 160, 719-727 (2003)

46. Mo E, H. Amin, I. H. Bianco and J. Garthwaite: Kinetics of a cellular nitric oxide/cGMP/phosphodiesterase-5 pathway. *J Biol Chem* 279, 26149-26158 (2004)

Key Words: cGMP, Cygnet, Membrane permeable peptides, Smooth muscle, NO, Natriuretic peptides, PKG

Send correspondence to: Dr Wolfgang Dostmann, Ph.D, University of Vermont, Department of Pharmacology, Health Science Research Facility 330, 149 Beaumont Avenue, Burlington, VT 05405-0075, USA, Tel: 802-656-0381, Fax: 802-656-4523, E-mail: wolfgang.dostmann@uvm.edu

http://www.bioscience.org/current/vol10.htm